Analysis of coupling controlled tunable Fano resonance in metal-insulator-metal plasmonic waveguide

RUKHSAR ZAFAR[1], YAZUSHA SHARMA[2]
[1]*Department of Electronics and Communication Engineering, Swami Keshvanand Institute of Technology, Management and Gramothan, Jaipur, India*
[2]*Department of Electronics and Communication Engineering, Jaipur Engineering College and Research Centre, Jaipur, India*

Fano resonance features a distinct asymmetrical profile caused by the interference of two resonant modes. The two resonant modes are termed “bright” and “dark” modes. In this paper, an analytical approach based on coupled mode theory (CMT) is used to demonstrate the tunable Fano resonance by varying the coupling between both the resonant modes. The effect on group delay, related bandwidth and dispersion characteristics is also explored. The results are validated through FDTD (finite-difference in Time Domain) by exciting a Fano resonance in Plasmonic MIM (Metal-Insulator-Metal) waveguide-based end-coupled stub resonators. The finding underscores the potential of Fano resonance in tuning dispersion, group delay etc., thus, it is viable in different photonics applications like sensing, modulation, and buffering.

(Received September 30, 2025; accepted June 2, 2026)

Keywords: Fano resonance, Coupled mode theory, FDTD, MIM waveguide

1. Introduction

Fano resonance is characterized by its unique asymmetric spectral profile [1]. The presence of a sharp peak and a deep dip in the profile makes it an ideal choice for switching and sensing applications [1-2]. The unique line shape arises from quantum interference between two distinct optical pathways: a narrow discrete resonance and a broad spectral continuum [2-3]. The interaction between these two resonances creates a noticeable abrupt spectral changeover, making Fano resonance distinct from the conventional symmetric resonance profiles [2-3]. The highly asymmetric, steep nature and the rapid transition between transmission minima and maxima allows for the development of energy-efficient optical modulators capable of fast state switching [4-5]. In sensing, the sharp gradient of the Fano dip enables the detection of extremely small environmental changes, offering sensitivity far superior to that of traditional resonance-based sensors [6-8]. It is particularly advantageous for wavelength de-multiplexing, where the narrow spectral features facilitate the precise separation of closely spaced optical channels [9-10]. Along with myriads of applications, Fano resonance profile is also viable in reducing the speed of light near resonance and strongly affects the phase response of the system, group delay and dispersion [11-12]. In recent years, plasmonics waveguide has emerged as the medium to facilitate Fano resonance due to interference between the bright mode (continuum of resonance) and the dark mode [8]. The bright mode is strongly coupled to the incoming signal whereas dark mode is weakly coupled to input radiation. The interaction between these modes results in asymmetrical resonance profile with large dispersion near resonance [8,10]. Plasmonics utilizes metal-insulator-metal (MIM) waveguide, metamaterials and nanoclusters to excite such a sharp asymmetrical profile. The enhanced near field and light-matter interaction in plasmonics waveguide make it as an ideal choice for Fano resonance excitement. Additionally, MIM waveguide also allows for deep sub-wavelength confinement [8,10]. Recent studies have demonstrated various structural strategies to excite and control Fano resonance in plasmonic systems. Khattak et al. proposed a hybrid waveguide structure that combines dielectric and plasmonic modes. In this structure, Fano resonance is excited for high-sensitivity sensing applications due to interference between long-range surface plasmon polariton (LRSPP) and dielectric waveguide modes [13]. Compact MIM-based geometries allow regulated interference between propagating and resonant modes, resulting in tunable Fano-like spectral characteristics in integrated photonic circuits, as demonstrated by Ebadi et al. [14]

By tailoring the parameters through structural design, plasmonic systems can achieve highly asymmetric and ultra-narrow spectral resonance. Also, Fano resonance has an asymmetrical profile which can be shaped or tuned by controlling the coupling between dark and bright mode. This work presents an analytical approach (Couple-mode-theory) to examine the impact of coupling between two modes, in shaping the asymmetrical resonance profile and optical phase. It also provides dynamic control over the phase, group delay, dispersion and the bandwidth for which delay remains constant. The transition between normal dispersion to anomalous dispersion is achieved by tuning the coupling strength. The plasmonic system is also investigated using numerical FDTD method to examine the effect of Fano resonance.

2. Analytical approach

Fano resonance is defined as the interaction between two states or modes which can be easily understood through the realm of coupled mode theory [15-16]. Considering two resonating modes α_1 *and* α_2, resonating at frequency ω_1 and ω_2. Coupling between modes can be governed by:

$$\frac{d\alpha_1}{dt} = -(j\omega_1 + \gamma)\,\alpha_1 + \Omega\alpha_2 + jk_1\,s_i$$
$$\frac{d\alpha_2}{dt} = -(j\omega_2 + \gamma)\,\alpha_2 + \Omega\alpha_1 + jk_2\,s_o \qquad (1)$$

$$s_o = cs_i + jk_1\,\alpha_1 + jk_2\,\alpha_2 \qquad (2)$$

here the term γ corresponds to decay rate, s_i and s_o are input and output flux entering and leaving the plasmonic waveguide system, Ω defines the coupling strength between two resonating modes while k_1 *and* k_2 are the coupling coefficients of modes α_1 *and* α_2 to the launched input field. In the general perception, one of the modes is considered as the bright (super-radiant) mode and other is considered as the dark (sub-radiant) mode. Bright mode is directly coupled to input radiation and results in broad super-radiant mode while dark mode is not connected to the input field directly ($k_2 = 0$) and hence results in narrow sub-radiant mode. ω_1 and ω_2 are the resonant frequency of bright and dark modes respectively. The intensity received at the output is governed by [16]:

$$\rho = \left|\frac{s_o}{s_i}\right|^2 = \left|\frac{{k_1}^2(j\omega_2 - j\omega + \gamma)}{(j\omega_2 - j\omega + \gamma)(j\omega_1 - j\omega + \gamma) + \Omega^2}\right|^2 \qquad (3)$$

The phase $\varphi(\omega)$ and term $\frac{d\varphi}{d\omega}$ for coupled modes can be computed as:

$$\varphi(\omega) = arg(j(\omega_2 - \omega) + \gamma) - arg\;(j(\omega_2 - \omega) + \gamma)(j(\omega_1 - \omega) + \gamma) + \Omega^2) \qquad (4)$$

$$\frac{d\varphi}{d\omega} = \frac{\gamma(2\Omega^2 + 2\omega^2 - 2\omega\omega_1 - 2\omega\omega_2 + {\omega_1}^2 + {\omega_2}^2 + 2\gamma^2)}{(\omega\omega_1 + \omega\omega_2 - \omega_2\omega_1 + \Omega^2 + \gamma^2 - \omega^2)^2 + \gamma^2(\omega_1 - 2\omega + \omega_2)^2} - \frac{\gamma}{\omega^2 - 2\omega\omega_2 + {\omega_2}^2 + \gamma^2} \qquad (5)$$

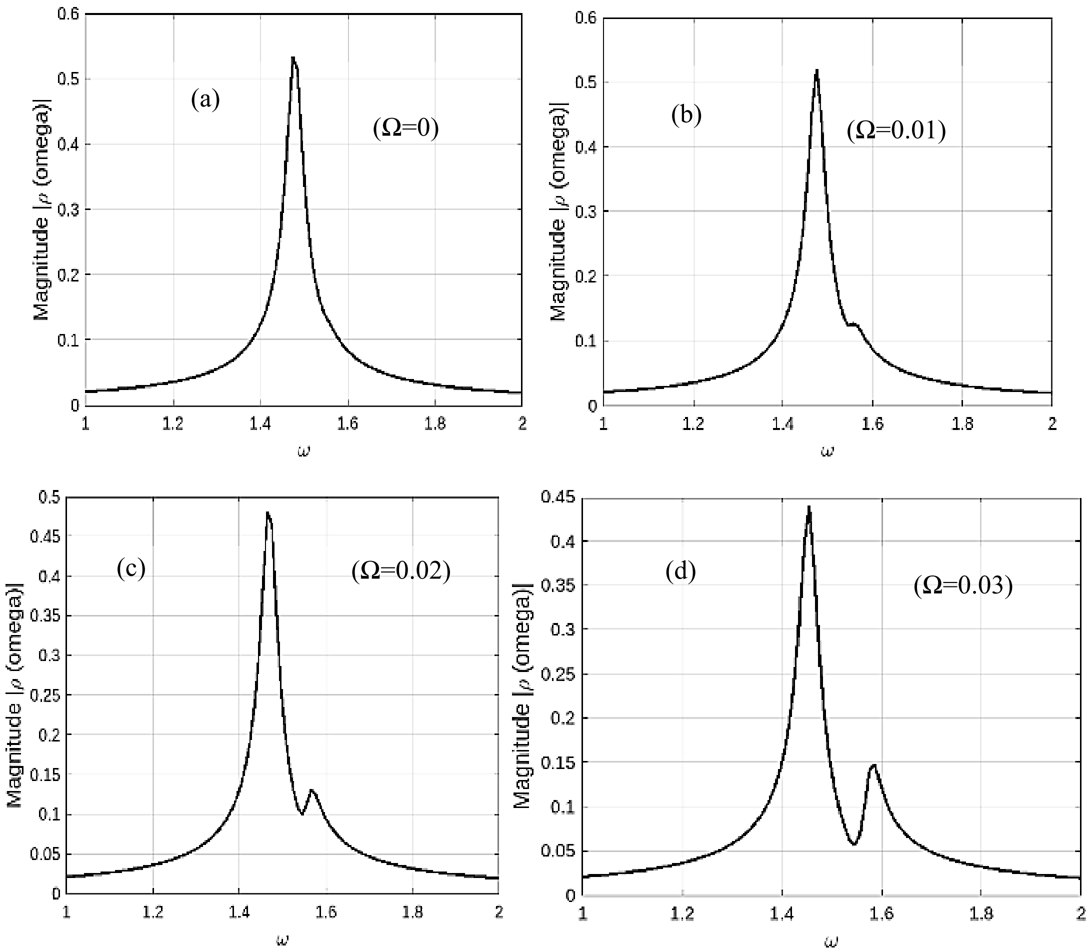

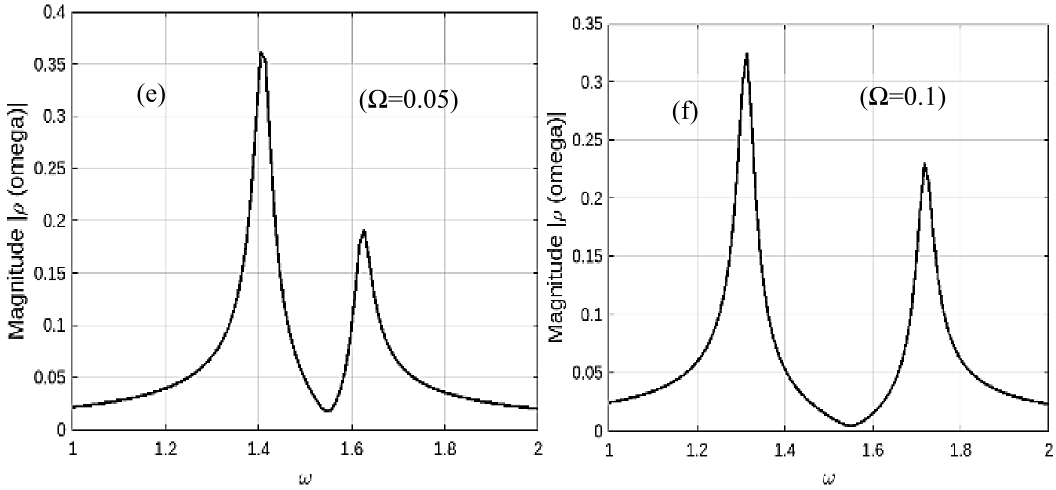

Fig. 1. Resonance characteristics (equation 3) for changing coupling coefficients (Ω). (The frequency is denoted in electron volt)

Fig. 1 shows the resonance profile for different coupling strength. Equation 3 depicts that the change in intensity (ρ) with coupling coefficient Ω. The fano resonance supports a unique resonance profile, in which resonance abruptly experiences a dip in the spectrum. As the coupling strength is increased, Fano profile experiences pronounced resonance splitting as illustrated in Fig. 1. The factors ω_2, ω_1 and, Ω play a crucial role in shaping the resonance profile as depicted in equation 4. The asymmetrical nature of Fano resonance for changing detuning factor ($\Delta\omega = \omega_2 - \omega_1$) and coupling coefficient Ω is studied using complex plane analysis through reflection argand diagram [16]. The variation of phase and $\frac{d\varphi}{d\omega}$ with respect to frequency (ω) as illustrated in Fig. 2 a, show a rapid and sharp phase variation which signifies a strong dispersion. The transition from positive phase to negative phase is crucial for achieving tunable group delay. Group delay (t_g) is defined by the term $\frac{d\varphi}{d\omega}$ and directly related to slow nature of light [12]. In the absence of coupling (Ω =0), group delay or $\frac{d\varphi}{d\omega}$ shows a single peak at the resonance representing strong field confinement and slow light at the resonance. As the coupling strength is further increased, the curve $\frac{d\varphi}{d\omega}$ begins to broaden near the zero-crossing.

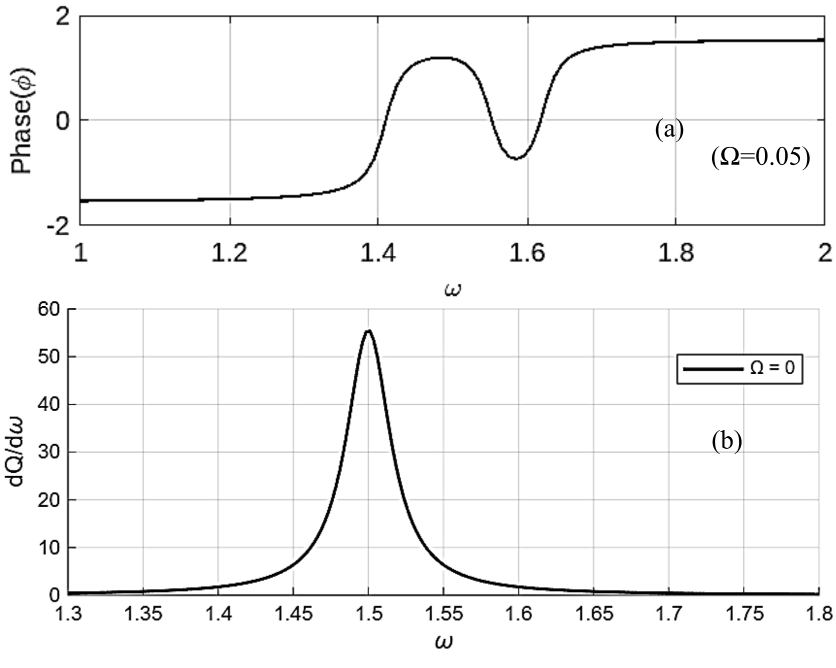

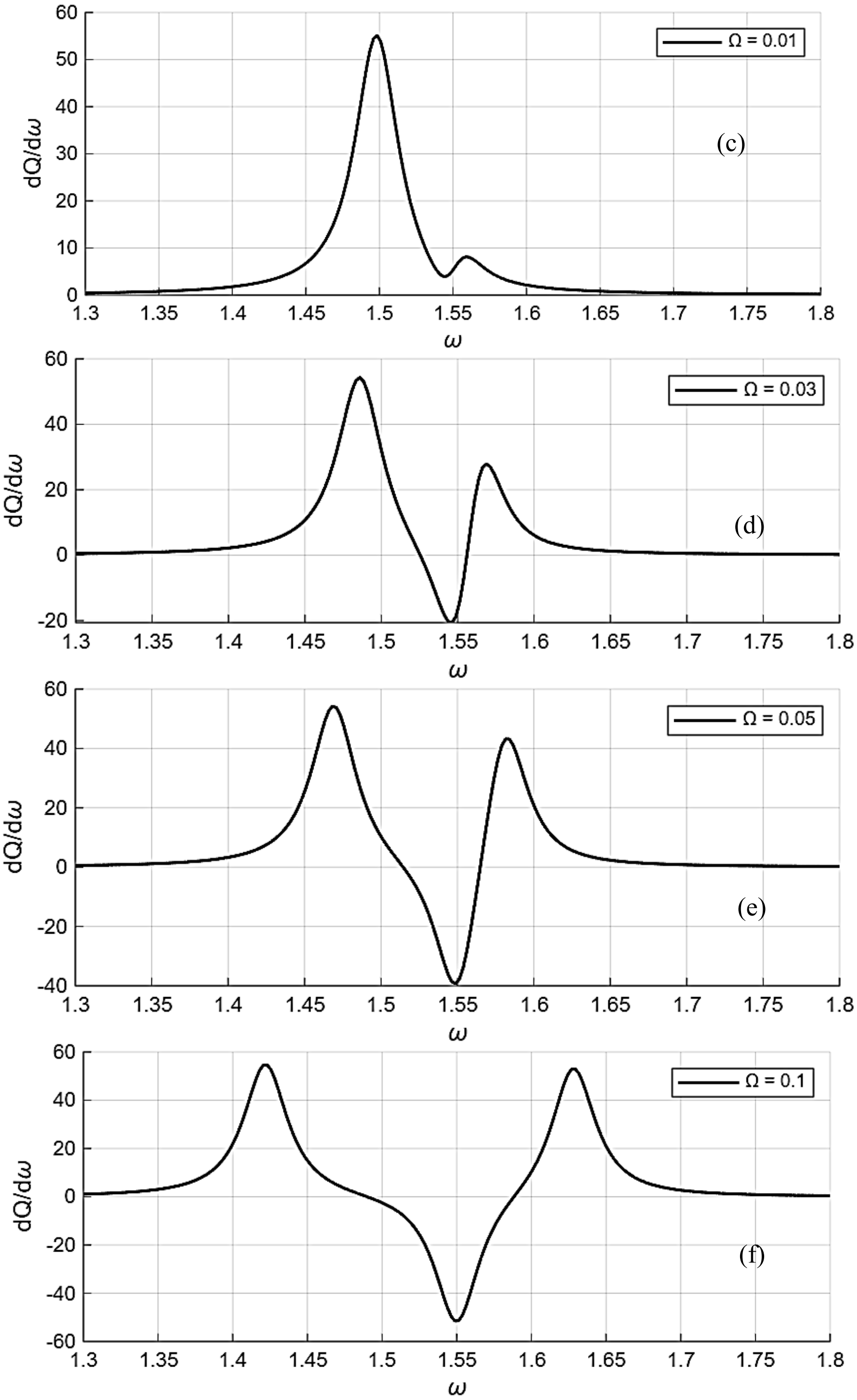

Fig. 2. (a) Phase of the Fano resonance characteristics computed at Ω=0.5; (b-g) Variation of group delay $(\frac{d\varphi}{d\omega})$ *as a function of angular frequency (ω) for changing value of coupling constant. The plots illustrate the influence of coupling strength on phase dispersion and slow-light characteristics*

This situation is ideal for slow light-based applications. The zero-crossing region is accompanied with the positive and negative value of $\frac{d\varphi}{d\omega}$. The slow light is generally accompanied by large dispersion. In the Fano resonance excited system, the normal dispersion $(\frac{d\varphi}{d\omega} > 0)$ or slow light effect changes to anomalous dispersion $(\frac{d\varphi}{d\omega} < 0)$. Thus, in a system of two connected resonators, the behavior of the group delay evolves characteristically as the coupling strength Ω increases. To illustrate the impact of coupling strength on group delay across different frequency, the contour map as shown in Fig. 3 is used.

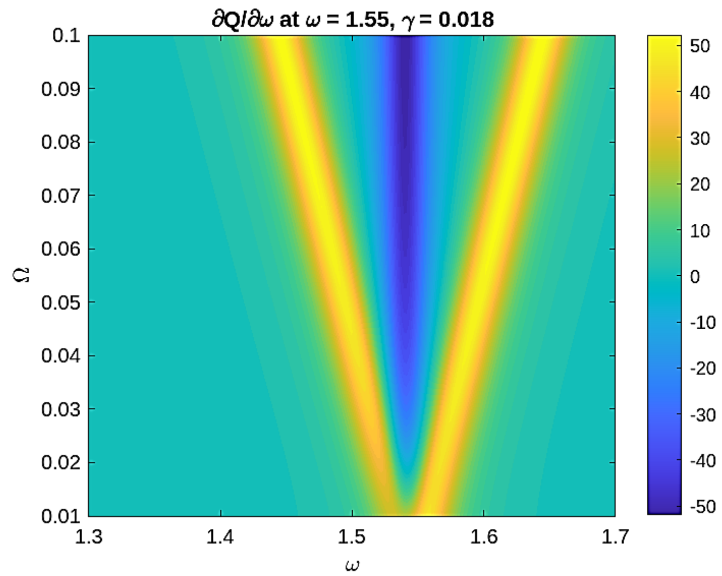

Fig. 3. Contour map illustrating the influence of coupling strength and resonance frequency on the dispersive characteristics of a Fano resonance-based photonic system. The plot highlights variations in dispersion behavior as a function of system parameters, demonstrating the tunability of the resonance profile and its impact on phase response and slow-light effects (colour online)

The V-shaped high-value zone for group delay is obtained for broader range of frequency as the coupling strength increases. The reason is quite evident as the splitting of mode is associated with higher dispersion or slow-light behavior. The blue area along the central frequency line indicates negative group delay or anomalous dispersion. Near the resonance, the normal dispersion region (positive slope) leads to slow light, as the pulse experiences a delay. Conversely, just beyond the resonance, the anomalous dispersion region (negative slope) causes the group delay to even become negative, resulting in fast light or pulse advancement. By dynamically tuning the coupling strength between the modes, one can control the position, shape of the Fano resonance, group delay and phase of the resonance profile, thereby enabling a smooth and tunable transition between slow and fast light regimes. In recent years, many artificial structured metamaterials have been designed to explore the tuning of Fano resonance and related group velocity of light [17]. In the next section, a plasmonic waveguide based coupled resonators are structured to illustrate the effect of Fano resonance and tunable group delay. However, a fundamental trade-off exists between group delay and loss in plasmonic waveguide and limit the practical usability of slow light regime. But, an optimal balance between group delay and loss ensures the usability of slow light based Plasmonics devices.

3. Simulation results

To study the effect of Fano resonance in photonics system, a Plasmonic MIM waveguide-based end coupled periodic stub resonators (as shown in Fig. 4-a) is analyzed using FDTD (Finite difference in Time domain) method. Perfectly matched boundary condition is used to minimize the effect of reflection from the end. The mesh grid size in x and z direction is chosen to be 5nm and time steps are governed through the relation $\Delta t = \frac{\Delta x}{2c}$ where c is the velocity of light in vacuum and Δx is mesh size. The metallic portion of plasmonic waveguide is silver whose characteristic is Drude-dependent and the parameter for model is [17]: $\epsilon_m(\omega) = \epsilon_\infty - \frac{\omega_p{}^2}{\omega^2 + i\gamma\omega}$; where ϵ_∞ (=3.7) is the dielectric constant at infinite angular frequency, ω_p(=9.1 ev) is the bulk plasma frequency, and γ (= 0.018 ev) is the electron collision frequency and ω is the angular frequency of the incident wave in vacuum. Insulating region is air. The width of both the bus waveguide and stub resonators is kept the same to deliver maximum power from bus waveguide to resonator. The input is p-polarized light, exciting SPP along the insulator-metal interface and propagating tightly along the narrow bus waveguide and couples the SPP in the resonator. Input signal directly couples with the lower resonator, but the upper resonator does not receive any signal directly from the waveguide, but it is excited by the signal coupled through lower resonator. Therefore, the mode excited by the lower resonator is known as bright resonant mode and mode in the upper resonator is termed as dark resonant mode. During the OFF-resonance condition, the incoming signal remains uncoupled in the resonator and propagates through BUS waveguide to the output port as depicted in Fig. 4-b. However, the signal coupled to the upper resonating system (related to dark mode resonance), also results in a transparent BUS waveguide (Fig. 4-c). This corresponds to the condition where reflectance suddenly drops to minimum value as depicted in the spectrum (Fig. 4-d) at dark mode resonance (λ=1303 nm). The phase response with respect to wavelength (shown in Fig. 4-e) depicts the steep rise and fall near the resonance. This is the consequence of interference between dark and bright resonant modes. The transition region of constant phase is also significant and can also be tuned by modifying the coupling distance between the resonators and results in smoother group delay profile. The simulated results are in line with the CMT results.

Thus, a single parameter, i.e. coupling distance between resonators can enable the control over phase, group delay and dispersion. This facilitates diverse applications in sensing, modulation, buffering etc. By controlling a single parameter i.e. coupling strength, a plasmonic system can be designed that features tailored slow-light effects and, optimized delay-bandwidth.

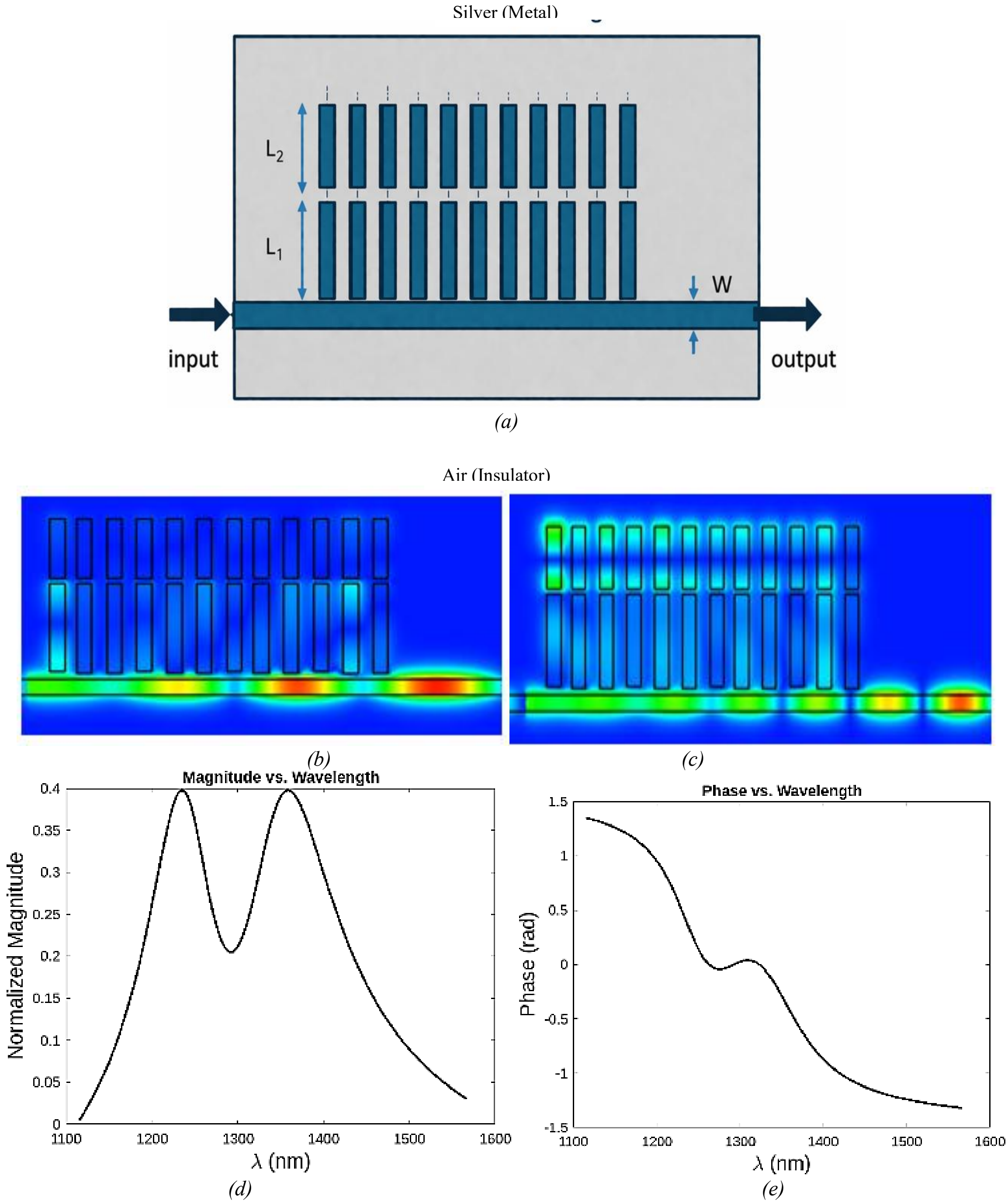

Fig. 4. (a) Schematic of MIM waveguide based end-coupled periodic stub resonators with following geometrical parameters (w=width of MIM waveguide and stub=50 nm, l_1= 240 nm & l_2= 150 nm is the length of lower and upper resonator respectively, gap between upper and lower resonator is maintained to 20 nm, (b-c) field profile at input wavelength λ=1550 nm and λ=1300 nm respectively; d) Reflected spectrum of MIM waveguide based end-coupled periodic stub resonators; e)Variation of Phase(rad) against input wavelength (colour online)

4. Conclusion

The work presented in this paper highlights the role of coupling between modes in shaping the Fano resonance characteristics. The Fano resonance possesses a distinct asymmetrical sharp resonance profile that results in reduced group velocity near resonance. Coupled mode theory is used to understand the behavior of coupling on resonance characteristics. The dynamic control over the coupling leads to transitions between slow and fast light regimes and tunes the phase response, group delay, and dispersion characteristics. It offers an extra degree of freedom and helps to tune the bandwidth over which group delay remains constant. This allows enhanced light-matter interaction over broader spectral ranges. The results are tested on Plasmonic MIM waveguide-based end-coupled periodic resonators using the FDTD method and are in line with the results obtained through CMT analysis.

References

[1] Mikhail F. Limonov, Advances in Optics and Photonics **13**(3), 703 (2021).
[2] Mikhail F. Limonov, Mikhail V. Rybin, Alexander N. Poddubny, Yuri S. Kivshar, Nature Photonics **11**(9), 543 (2017).
[3] Yong S. Joe, Arkady M. Satanin, Chang Sub Kim, Physica Scripta **74**(2), 259 (2006).
[4] Yingjie Xu, Lidan Lu, Bofei Zhu, Guang Chen, Jie Liao, Jin Zhang, Mingli Dong, Lianqing Zhu, Optics and Lasers in Engineering **187**, 108886 (2025).
[5] Joo Hwan Ko, J. H. Park, Y. J. Yoo, S. Chang, J. Kang, A. Wu, F. Yang, S. Kim, H. G. Jeon, Y. M. Song, Advanced Science **10**(32), 2304310 (2023).
[6] Songnan Chen, Yang Gao, Kangyao Sun, Qianyi Zhang, Zhehao Ye, Quanhong Fu, Yuancheng Fan, Fuli Zhang, Discover Applied Sciences **6**(1), 6 (2024).
[7] Hardik Mathuriya, Rukhsar Zafar, Ghanshyam Singh, IETE Journal of Research **69**(6), 3661 (2023).
[8] Yazusha Sharma, Rukhsar Zafar, IEEE Sensors Letters **7**(12), 1 (2023).
[9] Yang, Da-Jie, Song-Jin Im, Hai-Wen Huang, Chol-Song Ri, Kum-Dong Kim, Kil-Song Song, Ji-Cai Liu, and Qu-Quan Wang, Photonics Research **11**(8), 1423 (2023).
[10] Rukhsar Zafar, Pooja Chauhan, Mohammad Salim, Ghanshyam Singh, Plasmonics **14**(4), 1013 (2019).
[11] Fatemeh Kazemi, Optik **288**, 171189 (2023).
[12] Rukhsar Zafar, Yazusha Sharma, Ghanshyam Singh, Mohammad Salim, Optoelectron. Adv. Mat. **17**(7-8), 272 (2023).
[13] A. Khattak, L. Wei, Photonics **9**, 189 (2022).
[14] S. M. Ebadi, S. Khani, J. Örtegren, Optical and Quantum Electronics **56**, 910 (2024).
[15] Shanhui Fan, Wonjoo Suh, John D. Joannopoulos, Journal of the Optical Society of America A **20**(3), 569 (2003).
[16] Rukhsar Zafar, Mohammad Salim, Photonics and Nanostructures - Fundamentals and Applications **23**, 1 (2017).
[17] Rukhsar Zafar, Mohammad Salim, Infrared Physics & Technology **67**, 25 (2014).

*Corresponding author: rukhsarzafar1987@gmail.com